Numerical Analysis of Segmental Box Girder's Stress with Eccentric Tendon Anchoring on Balanced Cantilever Box Girder Bridge

Kevin Raenaldo[a*], M. Sigit Darmawan[a], Nur Ahmad Husin[a]

[a]*Departement of Civil Infrastructure Engineering,*
Sepuluh Nopember Institute of Technology, Surabaya, 60116, Indonesia
Corresponding author: k.raenaldo21@gmail.com

Abstract

Diagonal crack damage on the web of balanced cantilever box girder bridges has frequently occurred worldwide, including in Indonesia. Previous studies have shown that these cracks can result from additional shear stress caused by prestressed tendon anchoring. In this study, an analysis was conducted using a 2D element model verified through a numerical approach. The evaluation of box girder web stress values was used to assess the potential for cracking and confirm the results of crack mapping conducted on site. The research found that shear stress from prestressed tendon anchoring increases the total shear stress on the box girder web by up to 46.6% of the total shear stress value. The distribution of shear stress from prestressed tendon anchoring is concentrated in the anchoring areas on the top slab and bottom slab sides of the box girder web. The evaluation of principal tensile stress shows that the observed crack locations in the field correspond to areas where the principal tensile stress values exceed the allowable design limit.

Keywords: Anchorage zone; Box girder; FEM; Prestress; Shear stress

1. Introduction

Balanced cantilever box girder bridges have been widely used in modern bridge construction [1]. One such balanced cantilever bridge in Indonesia located in Java started service in 2017. However, in 2018, diagonal cracks were detected on the box girder web, as shown in Figure 1. Generally, cracks in the box girder web can lead to severe structural damage, reduce service life, and increase future maintenance costs [2].

On site crack mapping of bridges in Indonesia, as shown in Figure 2, resembles crack patterns caused by shear stress from prestressed tendons observed in a 2021 study (Figure 3) [3]. The horizontal shear stress effect on the box girder web due to eccentric tendon anchoring at the top and bottom fiber sections results in additional shear stress [4]. This effect cannot be detected by beam element analysis and is typically not considered in design. Principal tensile stress analysis was conducted using biaxial stress interaction, including normal stress from prestressing force and bending moment, as well as shear stress from tendon anchoring and external loads. Theoretical numerical approaches and finite element modeling were used for analysis. [5]

Figure 1. Cracks on a Bridge in Java Island, Indonesia.

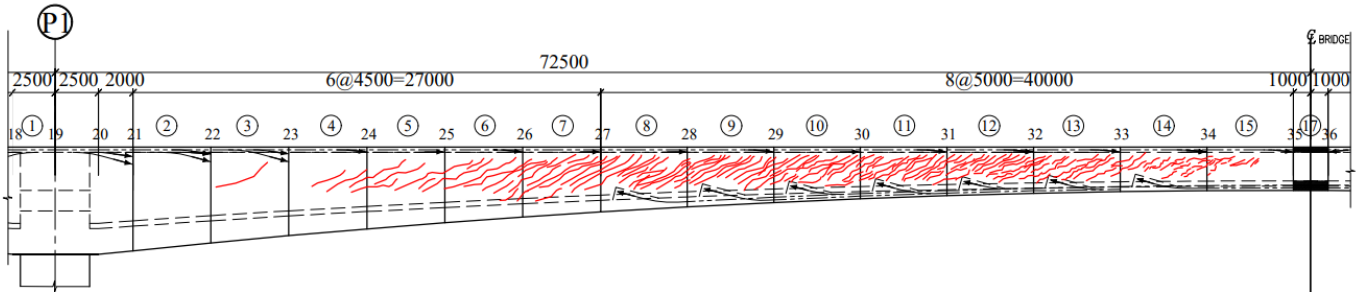

Figure 2. On Site Web Bos Girder Crack Pattern Mapping.

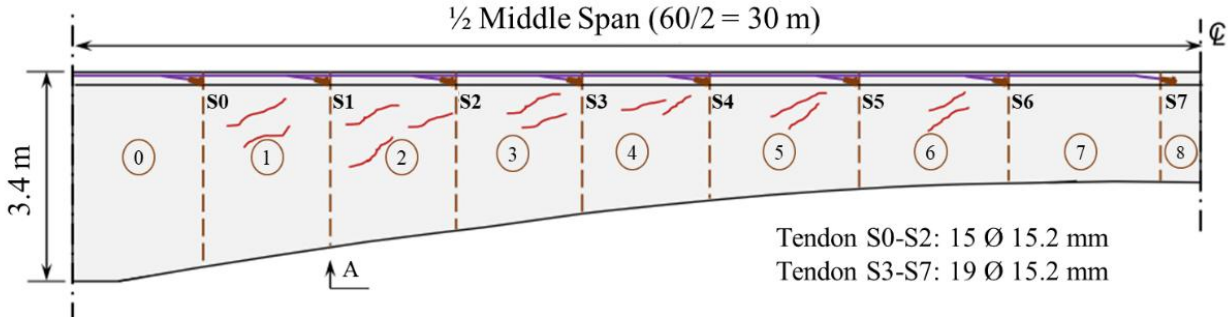

Figure 3. Crack Pattern Due to Horizontal Shear Stress on Web Box Girder [3].

Cracks that appear on the web box girder can occur due to several factors. Each contributing factor generally produces a specific crack pattern on the web [6] [7]. Previous studies have shown that cracks on the web can be caused by the addition of inadequate initial prestressing forces and the loss of significant prestressing forces due to concrete shrinkage and tendon relaxation [8]. Stresses due to temperature changes and temperature gradient differences [9]. Concentrated tensile stresses in areas of tendon eccentricity at the top and bottom of the box girder [10]. The negative effects of the biaxial stresses in the principal tensile stress on the web of the box girder [11]. As well as the effect of horizontal shear stresses on the web box girder due to eccentric tendon anchorage [3].

In this study, an evaluation of the influence of tendon eccentricity on the stresses in the cross-section of the box girder is conducted, which can cause cracks in the web of the box girder during construction, post-construction, and service under vehicle traffic loads. Thus, potential causes of cracking can be minimized and avoided in future bridge design stages.

2. Method

The research started with a literature study, including experimental research journals, proceedings, books, and allowable design specifications. The next stage involved collecting existing data on the bridges selected as research samples. Based on the existing data of the bridge, stress analysis was conducted on the web box girder, such as normal stress, shear stress, and principal tensile stress. The results of the analysis were then evaluated according to the stress limits of the design specification in Indonesia. The evaluation results will be used to confirm the cause of diagonal cracks in the bridge.

2.1.1. Existing Bridge Data

The existing bridge data used in this study includes as-built drawings and concrete material data. The studied bridge has 77+145+77 m spans with a balanced cantilever box girder superstructure. The analysis was carried out on the span P1-P2 of the bridge with a length of 145 m. Stress evaluation on the web box girder was carried out on half of the span P1 – P2. The longitudinal section and numbering of the segments and segment nodes of the bridge are shown in Figure 4.

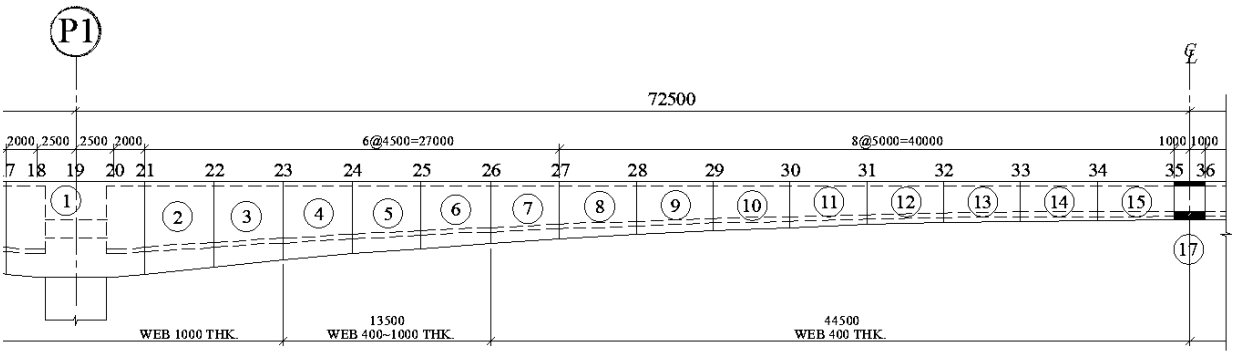

Figure 4. Longitudinal Section of the Bridge with Numbering of Segments and Segment Nodes.

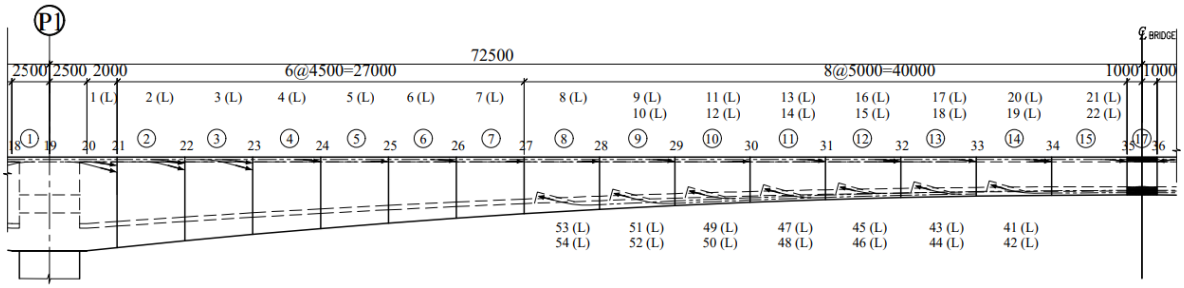

Figure 5. Longitudinal Section of the Bridge with Prestressed Tendon Configuration.

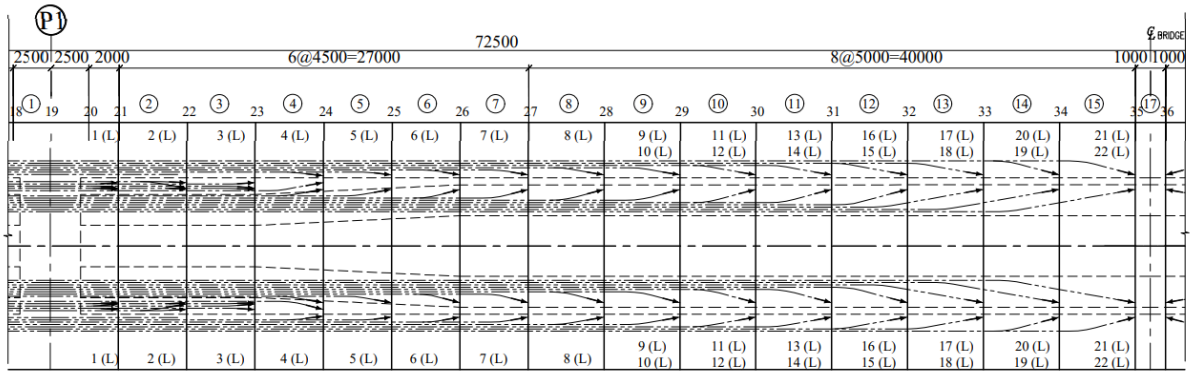

Figure 6. Cantilever Tendon Configuration of the Bridge Box Girder.

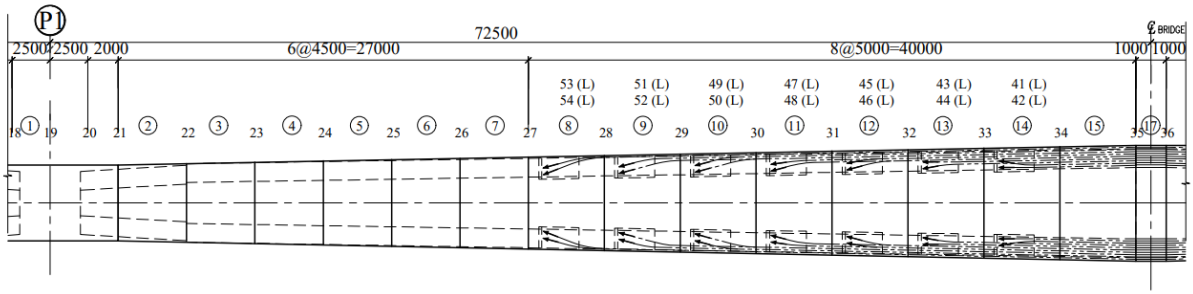

Figure 7. Continuous Tendon Configuration of the Bridge Box Girder.

The tendon configuration on the segment node cross-section is shown in Figure 5. The pre-stressed tendon configuration on the top and bottom sides of the box girder is shown in Figure 6 for the cantilever tendon on the top side and Figure 7 for the continuous tendon on the bottom side. In segments 8-14 or node segments 27-34, there is an overlap of prestressed tendon anchorage between the continuous tendon and the cantilever tendon of the bridge.

The concrete material of the bridge used in this study was taken from concrete core tests carried out during the bridge structure evaluation in 2022, as shown in Table 1. The concrete core test results of the bridge showed an average compressive strength of 42.64 MPa. This value is higher than the compressive strength value in the as-built drawing of the bridge, which is 41.5 MPa. However, there were two test samples with values below 75% of 41.5 MPa, specifically 31.3 MPa, so structurally, it still does not meet the concrete material acceptance requirements [12]. The Coefficient of Variation (CoV) value was obtained at 22%, indicating poor and inconsistent concrete work quality. Based on the

compressive strength test data, the compressive strength of the concrete used in the analysis is 30.21 MPa. This value is lower than the compressive strength in the as-built drawing of the bridge, which is 41.5 MPa.

Table 1. Compressive Strength of Bridge Concrete Material from Concrete Core Testing.

NoS	***Individual strength*** **f'$_c$ (MPa)**	***Average*** **f'$_c$ (MPa)**	***CoV*** **(%)**	***Actual*** **f'$_c$ (MPa)**
33	49.37, 60.12, 61.93, 43.04, 33.10, 32.47, 43.73, 40.55, 62.91, 58.41, **29.95**, 49.72, 50.97, 37.29, 36.94, 41.49, **27.95**, 49.65, 32.19, 49.65, 36.48, 42.65, 32.31, 33.93, 44.36, 37.34, 46.97, 50.77, 39.73, 34.91, 31.75, 44.36, 40.08	42.64	22	30.21

2.2. Numerical Analysis and Modeling

Numerical analysis and modeling of the box girder bridge were carried out to understand the distribution of stresses on the box girder segment. [13]. The numerical analysis was conducted using theoretical equations of stress values. The stresses on the box girder calculated in the numerical analysis include normal stress, shear stress, and principal tensile stress on the web box girder. The stresses on the web box girder are analyzed using the following equations.

1. Normal Stress Analysis

Normal stress on the web box girder is considered on the top and bottom sides of the web box girder in the horizontal direction along the length of the bridge [14]. The normal stresses caused by pre-stressing and external loads can be calculated using equation (1) [15].

$$f_{top,bot} = -\frac{F_{eff}}{A} \mp \frac{F_{eff}\, e\, y}{I} \pm \frac{M\, y}{I} \tag{1}$$

Where F_{eff} = effective prestressing force (N); A = cross-sectional area of the box (mm^2); e = eccentricity of the tendon (mm); y = distance from the top/bottom fiber of the web box girder to the centroid of the box section (mm); I = moment of inertia of the box section (mm^4); M = vertical moment (N.mm)

2. Shear Stress Analysis

Shear stress on the web box girder is considered according to the vertical loads on the bridge as in equation (3) and the additional shear stress due to the tendon prestress anchorage as in equation (4) [3]. Both shear stresses are summed as the total shear stress on the web box girder. The addition of these shear stresses is illustrated in Figure 8. The illustration of the total shear force on the web box girder shows that mathematically, the total shear stress on the web box girder can be calculated using equation (2). [16]

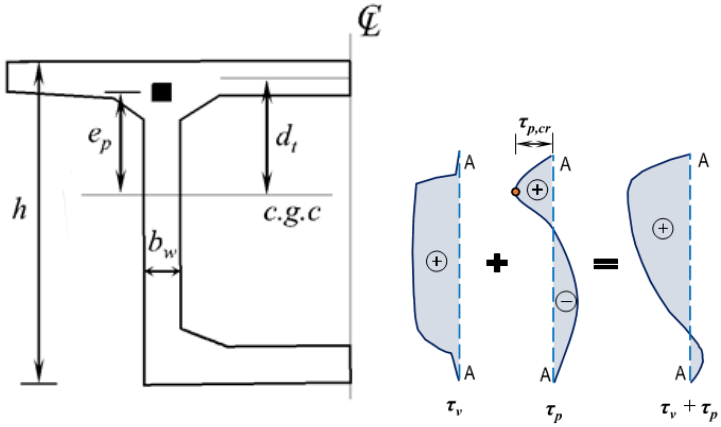

Figure 8. Illustration of Total Shear Force on the Box Girder Web [3].

$$\tau_{web} = \tau_v + \tau_p \tag{2}$$

$$\tau_v = \frac{VQ}{Ib_w} \tag{3}$$

$$\tau_p = \frac{9V_v}{2B_w h} = \frac{1.3\lambda P}{b_w h} \tag{4}$$

Where τ_v = shear stress due to vertical load (MPa); τ_p = shear stress due to tendon anchorage (MPa); V = vertical shear force (N); Q = first moment of area above the neutral axis (mm^3); I = moment of inertia of the section (mm^4); b_w = width of the web (mm); A = cross-sectional area of the box girder (mm^2); A_t = cross-sectional area of the top slab (mm^2); e_p = tendon eccentricity (mm); d_t = distance from the center of the top slab to the center of the box girder (mm); I = moment of inertia of the section (mm^4); b_w = width of the web (mm); h = height of the web (mm); P = anchoring force (N).

3. Principal Tensile Stress Analysis

Principal tensile stress on the concrete section is calculated by combining axial stress in the biaxial axis and shear stress using Mohr's Circle, as shown in Figure 9 [11]. Mathematically, the principal stress on the web box girder can be calculated using equation (5).

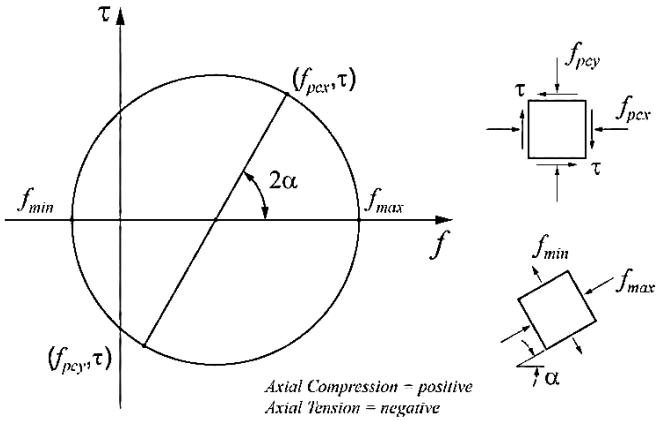

Figure 9. Concept of Principal Tensile Stress in Mohr's Circle [11].

$$f_{min} = \frac{f_x + f_y}{2} - \sqrt{\left(\frac{f_x - f_y}{2}\right)^2 + {\tau_{web}}^2} \tag{5}$$

Where f_x = normal stress in the horizontal direction (MPa); f_y = normal stress in the vertical direction (MPa); τ_{web} = maximum shear stress of the web (MPa). The value of f_y is used as 0 since there is no vertical prestress in the web box girder.

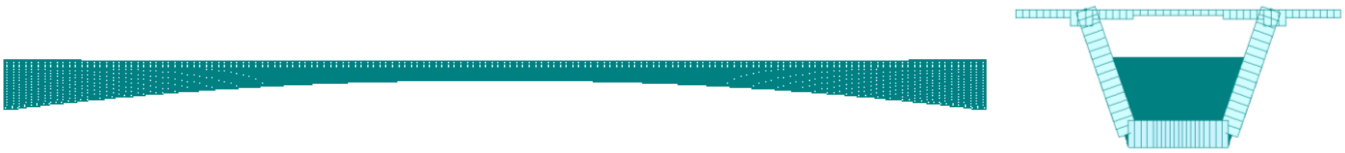

(a) (b)

Figure 10. Modeling of The Box Girder Bridge, (a) Long Section; (b) Cross Section.

Modeling of the box girder bridge is carried out using a 2D linear finite element model with Midas Civil software. The box girder elements are modeled using 2D linear shell elements, as seen in Figure 10. The boundary conditions are defined using fixed supports. The numerical analysis and model also consider the effects of construction staging that occur. The results of the construction staging analysis used for stress evaluation on the box girder segment consist of:

1. Output 1. Longest Cantilever in Construction Condition

This condition occurs after the installation of the last cantilever segment or before the closure segment casting of the bridge.

2. Output 2. Post-Construction Condition

This condition occurs after the casting of the closure segment, the installation of the continuous tendon, and the addition of the dead load of the bridge, such as asphalt and barriers.

3. Output 3. Vehicle Load Condition

This condition occurs during the service period of the bridge with 100% vehicle lane loading.

2.3. Stress Evaluation of Web Box Girder

The stress results of the web box girder from numerical analysis and modeling are evaluated according to the stress limits of the concrete material required by the design regulations in Indonesia. The allowable stress values of the web box girder are calculated based on the following references.

1. Normal Stress Evaluation

Normal stress is evaluated according to allowable stress limits required in [17]. The allowable stress value consists of two conditions: the transfer condition and the service condition. In the transfer condition, compressive and tensile stresses in the concrete section are not allowed to exceed the required values, where the compressive strength of concrete is used as 0.8 f'$_c$ in equation (6). With a concrete compressive strength (f'$_c$) of 30.21 MPa, the value of the compressive stress of the concrete material under transfer conditions is obtained in equation (7) and the allowable tensile stress in equation (8).

$$f'_{ci} = 0.8\, f'_c = 0.8\ 30.21 = 24.16\ MPa \tag{6}$$

$$f_{comp} = -0.6 f'_{ci} = -0.6\ 24.16 = -14.5\ MPa \tag{7}$$

$$f_{tens} = 0.25\sqrt{f'_{ci}} = 0.25\sqrt{24.16} = 1.23\ MPa \tag{8}$$

The allowable compressive stress in the transfer condition is calculated as -14.5 MPa, and the allowable tensile stress is 1.23 MPa. This allowable stress value is used in evaluating the normal stress of the web box girder at output 1 under construction conditions. Compressive and tensile allowable stresses under service conditions are calculated in equations (9) and (10).

$$f_{comp} = -0.45 f'_{ci} = -0.45\ 30.21 = -13.6\ MPa \tag{9}$$

$$f_{tens} = 0.5\sqrt{f'_{ci}} = 0.5\sqrt{30.21} = 2.75\ MPa \tag{10}$$

The allowable compressive and tensile stresses in the service condition are calculated in equations (9) and (10). The allowable compressive stress in the service condition is -13.6 MPa, and the allowable tensile stress is 2.74 MPa. These allowable stress values are used in the evaluation of normal stress in the web box girder for output 2 (post-construction condition) and output 3 (vehicle load condition).

2. Shear Stress Evaluation

Shear stress is evaluated according to the allowable shear stress required in [17]. With a compressive strength value for the bridge concrete (f'c) of 30.21 MPa, the value of the allowable shear stress for the concrete material is obtained in equation (11).

$$v_c = 0.3\sqrt{f'_c} = \ 0.3\sqrt{30.21} = 1.65\ MPa \tag{11}$$

The allowable shear stress is calculated as 1.65 MPa. This value is used in evaluating shear stress in the research

3. Principal Tensile Stress Evaluation

Principal tensile stress is evaluated to limit cracking on the web box girder in service conditions. Principal tensile stress is evaluated according to the tensile stress limit required in [18]. The ultimate tensile stress limit value is obtained in equation (12).

$$f_{lim} = 0.288\sqrt{f_c'} = 0.288\sqrt{30.21} = 1.59\ MPa \quad (12)$$

The allowable principal tensile stress of the concrete material is 1.58 MPa. This allowable stress value is used in the evaluation of the principal tensile stress and crack potential conducted in the study. The results of the principal tensile stress evaluation are compared with the crack pattern from field inspections. This comparison is used to confirm the effect of prestressed tendon anchorage can cause cracks in the web box girder. [11] [19].

3. Results and Discussion

The analyzed web box girder stress values were evaluated according to the concrete material allowable stress limits required in the specifications. The evaluated web box girder stresses include normal stress, shear stress, and ultimate tensile stress.

3.1. Normal Stress Evaluation of Web Box Girder

Normal stress in each cross-section of the box girder segment is reviewed under construction phase conditions, post-construction conditions without vehicle loads, and post-construction conditions with vehicle loads. The results of the normal stress analysis and evaluation are shown in Table 2.

Table 2. Normal Stress Evaluation of Web Box Girder.

Output	***Normal Stress***		***Node***														
			21	**22**	**23**	**24**	**25**	**26**	**27**	**28**	**29**	**30**	**31**	**32**	**33**	**34**	**35**
1	σx Total top	(MPa)	-0.21	-2.12	-1.94	-3.00	0.59	0.50	-2.04	-3.97	-7.21	-11.92	-16.99	-15.44	-17.19	-16.76	-16.91
	σx Total bot	(MPa)	-13.31	-13.38	-12.77	-12.39	-12.14	-11.95	-14.60	-13.06	-12.03	-10.69	-11.26	-12.45	-11.19	0.27	2.03
	f'lim	(MPa)	-14.50	-14.50	-14.50	-14.50	-14.50	-14.50	-14.50	-14.50	-14.50	-14.50	-14.50	-14.50	-14.50	-14.50	-14.50
	Comp Chk		***OK***	***OK***	***OK***	***OK***	***OK***	***OK***	***NOT OK***	***OK***	***OK***	***OK***	***NOT OK***	***NOT OK***	***NOT OK***	***NOT OK***	***NOT OK***
	f lim	(MPa)	1.23	1.23	1.23	1.23	1.23	1.23	1.23	1.23	1.23	1.23	1.23	1.23	1.23	1.23	1.23
	Tens Chk		***OK***	***OK***	***OK***	***OK***	***OK***	***OK***	***OK***	***OK***	***OK***	***OK***	***OK***	***OK***	***OK***	***OK***	***NOT OK***
2	σx Total top	(MPa)	-2.98	-4.49	-4.12	-4.98	-1.16	-0.97	-3.12	-4.53	-7.18	-11.24	-15.58	-13.30	-14.38	-13.39	-13.16
	σx Total bot	(MPa)	-10.27	-10.53	-9.97	-9.59	-9.26	-8.92	-11.41	-10.34	-9.88	-9.38	-11.05	-13.53	-13.56	-3.08	-2.22
	f'lim	(MPa)	-13.59	-13.59	-13.59	-13.59	-13.59	-13.59	-13.59	-13.59	-13.59	-13.59	-13.59	-13.59	-13.59	-13.59	-13.59
	Comp Chk		***OK***	***OK***	***OK***	***OK***	***OK***	***OK***	***OK***	***OK***	***OK***	***OK***	***NOT OK***	***OK***	***NOT OK***	***OK***	***OK***
	f lim	(MPa)	2.75	2.75	2.75	2.75	2.75	2.75	2.75	2.75	2.75	2.75	2.75	2.75	2.75	2.75	2.75
	Tens Chk		***OK***	***OK***	***OK***	***OK***	***OK***	***OK***	***OK***	***OK***	***OK***	***OK***	***OK***	***OK***	***OK***	***OK***	***OK***
3	σx Total top	(MPa)	-0.21	-2.12	-1.94	-3.00	0.59	0.50	-2.04	-3.97	-7.21	-11.92	-16.99	-15.44	-17.19	-16.76	-16.91
	σx Total bot	(MPa)	-13.31	-13.38	-12.77	-12.39	-12.14	-11.95	-14.60	-13.06	-12.03	-10.69	-11.26	-12.45	-11.19	0.27	2.03
	f'lim	(MPa)	-13.59	-13.59	-13.59	-13.59	-13.59	-13.59	-13.59	-13.59	-13.59	-13.59	-13.59	-13.59	-13.59	-13.59	-13.59
	Comp Chk		***OK***	***OK***	***OK***	***OK***	***OK***	***OK***	***NOT OK***	***OK***	***OK***	***OK***	***NOT OK***	***NOT OK***	***NOT OK***	***NOT OK***	***NOT OK***
	f lim	(MPa)	2.75	2.75	2.75	2.75	2.75	2.75	2.75	2.75	2.75	2.75	2.75	2.75	2.75	2.75	2.75
	Tens Chk		***OK***	***OK***	***OK***	***OK***	***OK***	***OK***	***OK***	***OK***	***OK***	***OK***	***OK***	***OK***	***OK***	***OK***	***OK***

The evaluation results of the web box girder normal stress under construction conditions (output 1) show that the maximum compressive stress value is -17.19 MPa at segment node 33 and the maximum tensile stress is 2.03 MPa at segment node 35. The compressive dan tensile stress value has exceeded the allowable normal stress value for concrete materials specified in the specification of -14.50 MPa (compression) and 1.23 MPa (tension). Overall, the evaluation results under these conditions show that the normal stress at segment nodes 27, 31, 32, 33, 34 and 35 exceeds the specified allowable stress limit. The evaluation is continued for the web box girder normal stress under post-

construction conditions (output 2). The maximum compressive stress value is obtained at -15.58 MPa at segment 31 node and the maximum tensile stress is 0 MPa. The compressive stress value has exceeded the allowable normal stress value for concrete materials specified in the specification of -13.59 MPa (compression) and 2.75 MPa (tension). Overall, the evaluation results under these conditions show that the normal stress at segment nodes 31 and 33 exceeds the specified allowable stress limit.

In the evaluation under vehicle service load conditions (output 3), it is found that the maximum compressive stress value is -17.19 MPa at segment node 33 and the maximum tensile stress is 2.03 MPa at segment node 35. The compressive stress value has exceeded the normal stress value allowed for concrete materials specified of -13.59 MPa (compression) and 2.75 MPa (tension). Overall, the evaluation results under these conditions show that the normal stress at segment nodes 27, 31, 32, 33, 34, and 35 exceeds the specified allowable stress limit.

3.2. Shear Stress Evaluation of Web Box Girder

Shear stress in each cross-section of the box girder segment is reviewed under construction phase conditions, post-construction conditions without vehicle loads, and post-construction conditions with vehicle loads. Shear stress on the web box girder consists of shear stress due to vertical loads and shear stress due to prestressed tendon anchorage. The results of the shear stress analysis and evaluation on the box girder element are shown in Table 3.

Table 3. Shear Stress Evaluation of Web Box Girder.

Output	***Shear Stress***		***Node***														
			21	**22**	**23**	**24**	**25**	**26**	**27**	**28**	**29**	**30**	**31**	**32**	**33**	**34**	**35**
1	τ DL max																0.26
	τ PS max	(MPa)	3.01	1.73	1.50	1.57	1.84	2.02	2.10	2.16	2.22	2.28	2.32	2.34	2.36	2.39	2.99
	τ Total max	(MPa)	3.18	2.40	2.35	2.59	3.32	4.40	5.22	5.36	5.46	5.43	5.22	4.80	4.18	3.45	3.14
	τ lim		1.65	1.65	1.65	1.65	1.65	1.65	1.65	1.65	1.65	1.65	1.65	1.65	1.65	1.65	1.65
	Shear Chk		***NOT OK***	***NOT OK***	***NOT OK***	***NOT OK***	***NOT OK***	***NOT OK***	***NOT OK***	***NOT OK***	***NOT OK***	***NOT OK***	***NOT OK***	***NOT OK***	***NOT OK***	***NOT OK***	***NOT OK***
2	τ DL max	(MPa)	1.68	1.48	1.43	1.62	2.05	2.78	3.40	3.44	3.43	3.30	3.01	2.54	1.88	1.10	0.26
	τ SDL max	(MPa)	0.29	0.27	0.28	0.35	0.48	0.66	0.80	0.82	0.84	0.76	0.65	0.48	0.48	0.28	0.07
	τ PS max	(MPa)	2.96	1.80	1.61	1.68	2.02	2.44	2.44	2.95	3.24	3.48	3.70	3.84	3.89	2.75	3.11
	τ Total max	(MPa)	3.08	2.57	2.59	2.85	3.74	5.29	6.27	6.78	6.96	6.85	6.61	6.20	5.81	4.09	3.30
	τ lim		1.65	1.65	1.65	1.65	1.65	1.65	1.65	1.65	1.65	1.65	1.65	1.65	1.65	1.65	1.65
	Shear Chk		***NOT OK***	***NOT OK***	***NOT OK***	***NOT OK***	***NOT OK***	***NOT OK***	***NOT OK***	***NOT OK***	***NOT OK***	***NOT OK***	***NOT OK***	***NOT OK***	***NOT OK***	***NOT OK***	***NOT OK***
3	τ DL max	(MPa)	1.68	1.48	1.43	1.62	2.05	2.78	3.40	3.44	3.43	3.30	3.01	2.54	1.88	1.10	0.26
	τ SDL max	(MPa)	0.29	0.27	0.28	0.35	0.48	0.66	0.80	0.82	0.84	0.76	0.65	0.48	0.48	0.28	0.07
	τ PS max	(MPa)	2.96	1.80	1.61	1.68	2.02	2.44	2.78	2.95	3.24	3.48	3.70	3.84	3.89	2.75	3.11
	τ LL max	(MPa)	0.31	0.27	0.29	0.37	0.51	0.72	0.91	0.96	1.00	1.01	0.98	0.89	0.74	0.57	0.25
	τ Total max	(MPa)	4.15	2.68	2.76	3.10	4.14	5.94	7.25	7.63	7.83	7.70	7.41	6.90	6.40	4.65	3.48
	τ lim		1.65	1.65	1.65	1.65	1.65	1.65	1.65	1.65	1.65	1.65	1.65	1.65	1.65	1.65	1.65
	Shear Chk		***NOT OK***	***NOT OK***	***NOT OK***	***NOT OK***	***NOT OK***	***NOT OK***	***NOT OK***	***NOT OK***	***NOT OK***	***NOT OK***	***NOT OK***	***NOT OK***	***NOT OK***	***NOT OK***	***NOT OK***

The evaluation results of the web box girder shear stress under construction conditions (output 1) show that the maximum shear stress value is 5.46 MPa at segment node 29. The shear stress due to tendon anchorage under these conditions has a value of 2.22 MPa and a percentage of 40.7% of the maximum shear stress that occurs in the web box girder. Under post-construction conditions (output 2), the maximum web box girder shear stress value is 6.96 MPa at segment node 29. This value has increased compared to the value during construction due to the installation of continuous tendons on the bottom slab and additional dead loads. The shear stress due to tendon anchorage under these conditions has a value of 3.24 MPa and a percentage of 46.6% of the maximum shear stress that occurs in the web box girder.

Under vehicle service load conditions (output 3), the maximum web box girder shear stress value is 7.83 MPa at segment node 29. The shear stress due to tendon anchorage under these conditions has a value of 3.24 MPa and a percentage of 41.4% of the maximum shear stress that occurs in the web box girder. The stress evaluation results show that the shear stress at all segment nodes starting from the construction phase, post-construction conditions to vehicle load conditions has exceeded the allowable stress limit 1.65 MPa.

3.3. Principal Tensile Stress Evaluation of Web Box Girder

The stress analysis results at each node of the web box girder segment are evaluated according to allowable stress limits specified. The stress evaluation is carried out at each construction stage from the construction phase (longest cantilever), post-construction phase, and vehicle load service phase of the bridge. The results of the principal tensile stress evaluation are shown in Table 4. The principal tensile stress evaluation results show that the maximum principal tensile stress value under construction conditions is 3.51 MPa at segment node 27. Under construction conditions (output 1), it is found that the principal tensile stress values at segment nodes 25, 26, 27, 28, 29, 30, 31, and 32 have exceeded the specified allowable stress limit of 1.59 MPa.

Table 4. Principal Tensile Stress Evaluation of Web Box Girder.

Output	***Principal Tens Str***		***Node***														
			21	**22**	**23**	**24**	**25**	**26**	**27**	**28**	**29**	**30**	**31**	**32**	**33**	**34**	**35**
1	fmin																-1.08
	fmin limit	(MPa)	-1.59	-1.59	-1.59	-1.59	-1.59	-1.59	-1.59	-1.59	-1.59	-1.59	-1.59	-1.59	-1.59	-1.59	-1.59
	Chk		***OK***	***OK***	***OK***	***OK***	***NOT OK***	***NOT OK***	***NOT OK***	***NOT OK***	***NOT OK***	***NOT OK***	***NOT OK***	***NOT OK***	***OK***	***OK***	***OK***
	2θ	*deg*	23.62	17.78	17.43	17.65	64.94	56.85	50.73	44.27	38.24	33.41	50.28	25.44	21.98	19.29	21.35
2	fmin	(MPa)	-1.89	-2.31	-2.51	-2.85	-4.04	-4.76	-4.95	-4.53	-3.99	-4.34	-6.05	-3.46	-3.10	-1.16	-0.84
	fmin limit	(MPa)	-1.59	-1.59	-1.59	-1.59	-1.59	-1.59	-1.59	-1.59	-1.59	-1.59	-1.59	-1.59	-1.59	-1.59	-1.59
	Chk		***NOT OK***	***NOT OK***	***NOT OK***	***NOT OK***	***NOT OK***	***NOT OK***	***NOT OK***	***NOT OK***	***NOT OK***	***NOT OK***	***NOT OK***	***NOT OK***	***NOT OK***	***OK***	***OK***
	2θ	*deg*	44.49	31.56	29.23	26.82	81.30	78.11	64.55	36.00	37.13	46.68	79.98	38.98	36.69	17.06	15.22
3	fmin	(MPa)	-3.99	-3.54	-3.66	-3.91	-5.18	-5.91	-6.08	-5.46	-4.75	-4.74	-6.71	-4.30	-4.15	-1.69	-2.06
	fmin limit	(MPa)	-1.59	-1.59	-1.59	-1.59	-1.59	-1.59	-1.59	-1.59	-1.59	-1.59	-1.59	-1.59	-1.59	-1.59	-1.59
	Chk		***NOT OK***	***NOT OK***	***NOT OK***	***NOT OK***	***NOT OK***	***NOT OK***	***NOT OK***	***NOT OK***	***NOT OK***	***NOT OK***	***NOT OK***	***NOT OK***	***NOT OK***	***NOT OK***	***NOT OK***
	2θ	*deg*	85.37	52.57	45.08	37.60	65.69	89.39	30.76	32.42	34.68	44.71	78.87	45.57	48.15	15.65	12.30

Under post-construction conditions (output 2), the maximum principal tensile stress value is 6.05 MPa at segment node 31. Under post-construction conditions, it is found that the principal tensile stress values at segment nodes 21, 22, 23, 24, 25, 26, 27, 28, 29, 30, 31, 32, 33, and 34 have exceeded the specified allowable stress limit of 1.59 MPa. Under vehicle load service conditions (output 3), the maximum principal tensile stress value is 6.71 MPa at segment node 31. Under vehicle load service conditions, it is found that the principal tensile stress values at segment node 21, 22, 23, 24, 25, 26, 27, 28, 29, 30, 31, 32, 33, and 34 have exceeded the specified allowable stress limit of 1.59 MPa.

3.4. Crack Evaluation of Web Box Girder

The stress evaluation results on the web box girder show that the shear stress and principal tensile stress values have exceeded the specified allowable stress limits. The comparison of the principal tensile stress evaluation results with the crack pattern mapping from site inspections is shown in Figure 2 and Table 4. The crack evaluation on the web box girder shows that the crack location corresponds to the segment node location which has a principal tensile stress value exceeding the allowable stress limit. Under construction phase conditions (output 1), it is found that the principal tensile stress that occurs in the web box girder segment nodes 25, 26, 27, 28, 29, 30, 31 and 32 have exceeded the specified allowable stress limit. This indicates that initial cracks in the web box girder segment nodes have occurred during construction. [20]

The evaluation under post-construction conditions (output 2) shows that other box girder segment node locations have been found to exceed the allowable stress limit. This occurs due to the addition of the continuous tendon anchorage and additional bridge dead load. The crack location on the web box girder can be specifically shown by the principal tensile stress diagram that occurs at each output as shown in Table 5. The purple line shows the principal tensile stress value, and the red dashed line shows the specified allowable principal tensile stress limit.

The principal tensile stress diagram shows an increase in principal tensile stress in the web box girder height dimension as the bridge condition changes from the construction phase to the bridge service phase. If the principal tensile stress diagram is compared with the crack mapping results, it is found that:

1. At segment node 25, the principal tensile stress value that exceeds the allowable limit is located on the top side of the web box girder at a height of 1100 mm from the top support of the web box girder. This condition is in accordance with the field crack mapping results that the crack at segment node 25 appears on the top side of the web box girder.
2. At segment node 29, the principal tensile stress diagram shows a principal tensile stress value that exceeds the allowable limit located at the entire height of the web box girder. This condition is in accordance with the field crack mapping results that the crack at segment 29 node appears on almost the entire web box girder.

Overall, the crack formation process of the diagonal web box girder of the bridge under study begins with the shear stress distribution of web box girder during the construction phase which is concentrated on the top side of the web. This shear stress is largely contributed by the top prestressed tendon anchorage as shown in Table 3. Under post-construction conditions, a new stress concentration appears on the underside of the web due to continuous tendon anchorage. The tendon anchorage on the underside acts to add to the shear stress that has occurred on the web during construction. The shear stress concentration that occurs increases the principal tensile stress value of the web box girder to exceed the specified allowable limit. This condition has led to the appearance of the first diagonal crack in the web box girder.

The main factor causing the diagonal cracks in the web is insufficient design thickness of the web box girder. The web box girder at segment nodes 26 - 35 with a thickness of 400 mm does not have sufficient allowable shear stress capacity to accommodate the shear stress that occurs due to vertical loads and additional shear stress from prestressed tendon anchorage. This occurs because generally in the cross-section of the segment in the middle of the span, the thickness of the web box girder is minimized to reduce the weight of the segment. [21].

Table 5. Principal Tensile Stress Diagram of Web Box Girder.

Output	Output 1	Output 2	Output 3
Node 25	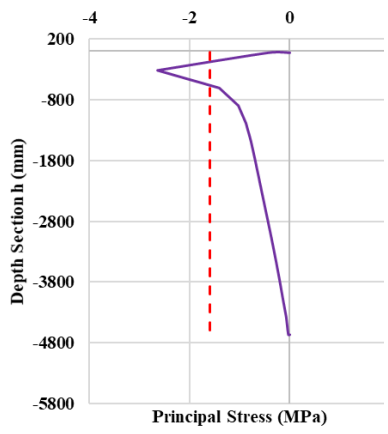	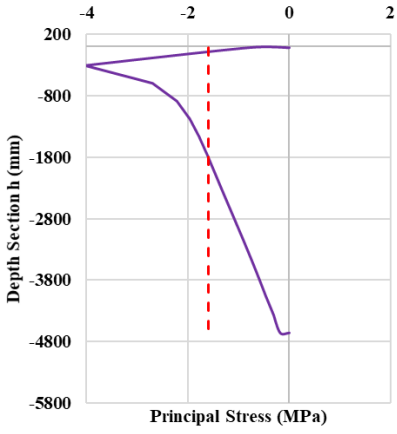	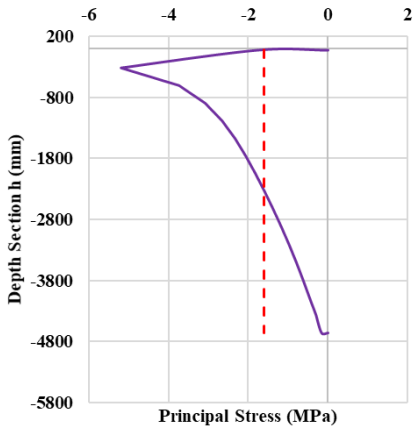
Node 29	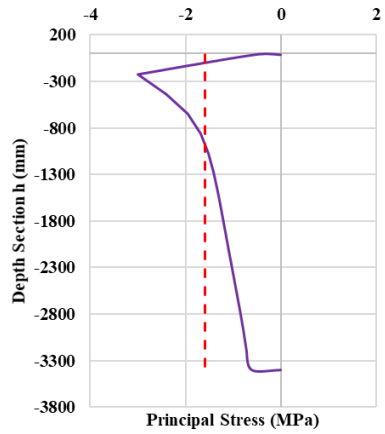	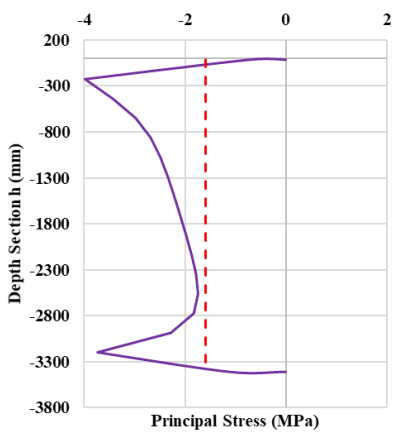	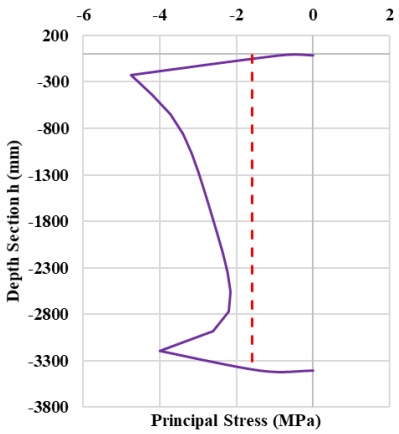

4. Conclusions

Based on the analysis and evaluation conducted, the evaluation results of normal stress, shear stress and principal tensile stress show that there are segment nodes with stress values during construction to service that have exceeded the allowable stress limits specified in the design specification. The prestressed tendon anchorage causes a concentrated shear stress distribution on the prestressed tendon anchorage side of the top and bottom of the web box girder. The most critical shear stress distribution on the web box girder occurs in segments with eccentric tendon overlap on the top slab and bottom slab of the cross-section. This occurs because generally in the cross-section of the middle span segment, the thickness of the web box girder is minimized to reduce the weight of the segment. The contribution of shear stress due to prestressed tendon anchorage in the middle span segment up to 46.6% of the total shear stress of the web box girder.

The crack potential evaluation results show the locations of segment nodes with shear stress and principal tensile stress values that exceed the allowable stress limits in accordance with the results of the crack pattern mapping on site. This indicates that the concentration of shear stress and principal tensile stress due to prestressed tendon anchorage has caused diagonal cracks in the web box girder.

Acknowledgment

This research was funded by the Ministry of Research and Culture of Indonesia, through the BIMA Kemendikbud program, 2024. We express our gratitude for their support and contribution. The authors sincerely thank the "Laboratory of Building Materials and Structures" for their invaluable support.

References

[1] V. Heggade, "Segmental precast technology for multi-span bridges," in *Multi-Span Large Bridges*, 2015, pp. 673-700.

[2] H. Huang, S.-S. Huang and K. Pilakoutas, "Modeling for assessment of long-term behavior of prestressed concrete box-girder," *Journal of Bridge Engineering,* vol. 3, p. 23, 2018.

[3] Z.-Q. He, M. Tang, T. Xu, Z. Liu and Z. Ma, "Additional Shear Stresses in Webs of Segmental Concrete Bridges Due to Anchorage of Cantilever Tendons," *Journal of Bridge Engineering,* vol. 26, 2021.

[4] Z.-Q. He, Y. Li, T. Xu, Z. Liu and Z. Ma, "Crack-based serviceability assessment of post-tensioned segmental concrete box-girder bridges," *Structures,* 2021.

[5] R. Malm and A. Ansell, "Crack formation in two segmentally constructed balanced cantilever box- girder bridges," *Proc., fib Symp. 2012: Concrete Structures for Sustainable Community,* pp. 151-154, 2012.

[6] W. Podolny, "The Cause of Cracking in Post-Tensioned Concrete Box Girder Bridges and Retrofit Procedures," *PCI Journal,* vol. 30, pp. 82-139, 1985.

[7] W. Podolny, "Evaluation of Transverse Flange Forces Induced by Laterally Inclined Longitudinal Post-Tensionin in Box Girder Bridges," *PCI Journal,* vol. 31, pp. 44-61, 1986.

[8] Z. Kamaitis, "The causes of shear cracking in prestressed concrete box-girder bridges," *Journal of Civil Engineering and Management,* vol. 2, pp. 26-34, 1996.

[9] R. Malm, "Shear cracks in concrete structures subjected to in-plane stresses," *Ph.D. thesis, Dept. of Civil and Architectural Engineering Royal Institute of Technology,* 2006.

[10] R. Malm and H. Sundquist, "Time-dependent analyses of segmentally constructed balanced cantilever bridges," *Engineering Structures,* vol. 32, 2010.

[11] A. Okeil, "Allowable Tensile Stress for Webs of Prestressed Segmental Concrete Bridges," *ACI Structural Journal,* pp. 488-495, 2006.

[12] ACI, ACI 318-2019 : Building Code Requirements, Farmington Hills, MI 48331 USA: American Concrete Institute, 2019.

[13] G. Wang, X. Jun and F. Yufang, "Investigation on Crack of Long-span Prestressed Concrete Box Girder Bridges in Service," *Journal of Highway and Transportation Research and Development (English Edition),* vol. 4, no. 1, pp. 71-76, 2009.

[14] C. Zhao, Y. Zhou, X. Zhong, G. Wang, Q. Yang and X. Hu, "A Beam-Type Element for Analyzing The Eccentric Load Effect of Box Girder Bridges," *Structures vol 36,* pp. 1-12, 2022.

[15] FHWA, Post-Tensioned Box Girder Design Manual, Washington: Federal Highway Administration, 2016.

[16] Z.-Q. He, H. Hong, Z. Liu and Z. Ma, "Three-Dimensional Spreading of Prestressing Forces in Box Girders," *Structures,* vol. 33, 2021.

[17] BSN, RSNI T-12-2004 : Perencanaan struktur beton untuk jembatan, Jakarta, Indonesia: Badan Standardisasi Nasional , 2004.

[18] AASHTO, AASHTO LRFD Bridge Design Specifications 9th edition., Washington DC: American Association of State Highway and Transportation Officials, 2020.

[19] A. J. Notkus and Z. Kamaitis, "Evaluation of shear stresses in the webs of segmental box-girder concrete bridges," *Statyba,* vol. 5, no. 1, pp. 47-52, 1999.

[20] D. Huang and B. Hu, "Evaluation of Cracks of Hathaway Precast concrete Segmental Box Girder Bridge," *IABSE Congress Report,* 2012.

[21] X. Wu, J. Li, X.-S. Yi and Z.-C. Zhang, "Analysis of Box Girder Cracks on PC Bridge," in *2014 International Conference on Mechanics and Civil Engineering*, Wuhan, China, 2014.